Siddiqui, T., Stolle, C., Lühr, H., Matzka, J. (2015): On the relationship between weakening of the northern polar vortex and the lunar tidal amplification in the equatorial electrojet. - *Journal of Geophysical Research*, *120*, 11, pp. 10006—10019.

DOI: http://doi.org/10.1002/2015JA021683

AGU PUBLICATIONS

JGR

Journal of Geophysical Research: Space Physics

RESEARCH ARTICLE
10.1002/2015JA021683

Key Points:
- Semimonthly lunar modulation of the EEJ shows enhancements around the time of PVW
- The peak semimonthly lunar tidal amplitudes show correlation with the reversed zonal wind speed
- The timings of lunar tidal peak and PVW show better correlation than their respective magnitudes

Supporting Information:
- Supporting Information S1

Correspondence to:
T. A. Siddiqui,
tarique@gfz-potsdam.de

Citation:
Siddiqui, T. A., C. Stolle, H. Lühr, and J. Matzka (2015), On the relationship between weakening of the northern polar vortex and the lunar tidal amplification in the equatorial electrojet, *J. Geophys. Res. Space Physics*, *120*, 10,006–10,019, doi:10.1002/2015JA021683.

Received 15 JUL 2015
Accepted 22 OCT 2015
Accepted article online 26 OCT 2015
Published online 18 NOV 2015

On the relationship between weakening of the northern polar vortex and the lunar tidal amplification in the equatorial electrojet

Tarique A. Siddiqui[1,2], Claudia Stolle[1,2], Hermann Lühr[1], and Jürgen Matzka[1]

[1]GFZ German Research Centre for Geosciences, Potsdam, Germany, [2]Institute of Earth and Environmental Science, University of Potsdam, Potsdam, Germany

Abstract Enhanced lunar tidal effects in the equatorial electrojet (EEJ) during northern winters in the form of "big L" days have been known for a long time. Recent studies suggest that the changes in the tidal propagation conditions due to stratospheric sudden warmings could be responsible for this phenomenon. In this work we have used the *H* component of the magnetic field recorded at Huancayo from 1997 to 2013 to study the relation between the timing and magnitude of the semimonthly lunar tide in the EEJ and the stratospheric polar vortex weakening (PVW). We prefer a definition of PVW by taking into account the atmospheric conditions from December to February for each winter. Our results indicate that the semimonthly lunar tide in the EEJ gets enhanced during northern winters when a significant PVW occurs and its peak timing and magnitude is correlated with the timing and intensity of PVW. The timing of lunar tidal peaks and PVW correlate better than their respective magnitudes. Our results suggest that the initiation of the lunar tidal enhancement in most of the cases is closely related to a PVW event. Furthermore, we discuss events where the semimonthly lunar tidal enhancements are not well timed with respect to PVW. We also suggest that the amount of tropospheric forcing into the stratosphere plays a major role in the enhancement of the lunar tides in the EEJ.

1. Introduction

Lunar tidal enhancement in the equatorial electrojet (EEJ) in relation to stratospheric sudden warming (SSW) events have been studied extensively in recent years [e.g., *Stening*, 2011; *Park et al.*, 2012; *Lühr et al.*, 2012; *Yamazaki et al.*, 2012; *Yamazaki*, 2013; *Siddiqui et al.*, 2015]. Large lunar effects in the EEJ between November and March were first reported by *Bartels and Johnston* [1940], but the mechanism behind these observations were not fully understood. Recent publications have tried to explain this phenomenon through the enhanced planetary wave (PW) activity which is assumed to be responsible for causing SSW [*Matsuno*, 1971]. *Forbes and Zhang* [2012] explained the amplified lunar tidal winds in the ionospheric dynamo region during an SSW through the changes in the zonal mean zonal wind and temperature of the middle atmosphere which shifts the atmospheric (Pekeris) resonance peak onto the lunar period (12.42 h). Subsequently, the amplification of the semimonthly lunar tide in the EEJ during SSW winters were reported by *Yamazaki* [2013] to be almost three times larger compared to the non-SSW winters.

SSWs have been studied quite extensively since they were first observed by *Scherhag* [1952]. SSWs are characterized by the weakening of the westerly winds in the northern stratosphere and a breakdown of the polar vortex which leads to a sudden rise in the polar stratospheric temperature by several tens of degrees [e.g., *Andrews et al.*, 1987] and are usually classified into major and minor warming events. According to the World Meteorological Organization (WMO) definition, an SSW is identified as a major warming event if there is a reversal of the latitudinal temperature gradient poleward of 60°N and the reversal of the zonal mean zonal wind at 60°N/10 hPa and as a minor warming if there is an increase in the stratospheric temperature by 25 K or more within a week without the reversal of the zonal mean zonal wind. Moreover, different authors have also used modified versions of the WMO definition and other diagnostic variables to identify SSWs. For example, *Charlton and Polvani* [2007] used solely the wind reversal criterion to detect major SSWs. *Martineau and Son* [2013] identified SSWs based on the NAM (Northern Annular Mode) index at 10 hPa. Empirical orthogonal functions (EOFs) of gridded pressure-level data of geopotential height anomalies or zonal wind anomalies have been employed by *Baldwin and Dunkerton* [2001] and *Limpasuvan et al.* [2004], respectively, to identify

SSWs. The availability of numerous diagnostics has created a situation where there are at the moment many different ways to detect SSWs, but there is an ambiguity in choosing the most suitable one. For more extensive information on the various SSW definitions that have been used in the literature, the readers may refer to *Butler et al.* [2015].

Recently, *Zhang and Forbes* [2014] defined the concept of Polar Vortex Weakening (PVW) by using measurements of the mean zonal wind (U) at 70°N/48 km altitude and the zonal mean temperature (T) at 90°N/40 km, which showed good correlation between the timing and magnitude of PVWs and the M_2 lunar tide at 110 km altitude. The lunar tide was determined from the temperature measurements made by the SABER (Sounding of the Atmosphere using Broadband Emission Radiometry) instrument on board the Thermosphere Ionosphere Mesosphere Energetic Dynamics satellite between ±50° latitude. *Chau et al.* [2015] used this definition of PVW to demonstrate the correlation between the timing of PVW and enhancement of lunar tides in the upper mesosphere, lower thermosphere (MLT) by using wind data from middle- and high-latitude stations. However, they reported some observations where the correlation failed when the M_2 enhancement occurred much earlier than the defined PVW days for those years.

In this paper we use a PVW definition similar to the one put forward by *Zhang and Forbes* [2014] to demonstrate a correlation between the timing and peak magnitude of PVW and the semimonthly lunar tidal modulation of the equatorial electrojet (EEJ) as estimated from the Huancayo magnetic observatory for the years 1997–2013. We also report two observations where the correlation breaks down and the semimonthly lunar tide in the EEJ enhances much earlier than the PVW day in these cases.

The structure of this paper is as follows. Section 2 describes the various data sets used in this study. In section 3, we introduce our approach for determining the strength of the lunar tidal modulation of the equatorial electrojet. In section 4, we present our observations followed by discussion in section 6. The conclusions from this work is presented at the end.

2. Data Set

Recordings of hourly means of the horizontal component, H of the geomagnetic field at Huancayo, HUA, (−12.05°N, 284.67°E; magnetic latitude: −0.6°) and San Juan, SJG, (18.11°N, 293.85°E; magnetic latitude: 28.31°) are available for the period 1997–2013 and from 1997 to 2011 for Fuquene, FUQ, (5.47°N, 286.26°E; magnetic latitude: 18.12°) at the World Data Centre (WDC) for Geomagnetism, Edinburgh. Our study is limited to the above mentioned time intervals since the FUQ data are presently not available after 2011 and HUA data are missing at the WDC for the years 1970–1996.

To consider the dependence of the EEJ strength on solar activity, we use the solar flux values $F_{10.7}$ in solar flux unit (sfu: 10^{-22} W m^{-2} Hz^{-1}) which are available at the GSFC/SPDF OMNIWeb interface at http://omniweb.gsfc.nasa.gov. To remove the ring current effect, the *Dst* index (availabe at the WDC for Geomagnetism, Kyoto) has been used for the period 1997–2013.

For quantitatively defining the weakening of the northern polar vortex, we use the MERRA (Modern-Era Retrospective Analysis for Research and Application) data (ftp://goldsmr3.sci.gsfc.nasa.gov/data/s4pa/MERRA/).

3. Methods of Analysis

3.1. Lunar Tide Identification in Magnetic Ground Station Records

The lunar semidiurnal component (M_2) dominates the lunar tidal effects in magnetic records. The M_2 tide shows a semimonthly variation (14.77 days) at a fixed local time. The lunar tidal modulation of the equatorial electrojet related to stratospheric sudden warming has been estimated using the horizontal component of the geomagnetic field, H, e.g., at Huancayo [*Siddiqui et al.*, 2015] and Addis Ababa [*Yamazaki et al.*, 2012] in recent literature.

Both these studies employed different procedures to remove the effects of large-scale magnetospheric currents in H. While the former study used a reference observatory at some distance away from the dip equator to remove these effects [e.g., *Manoj et al.*, 2006], the latter one subtracted the *Dst* index from H.

The two studies also differed regarding the definition of the EEJ strength. The method used by *Siddiqui et al.* [2015] eliminates some contributions of the S_q currents from the recordings of the equatorial observatory while calculating the EEJ strength, whereas in the method used by *Yamazaki et al.* [2012] the S_q contributions are retained.

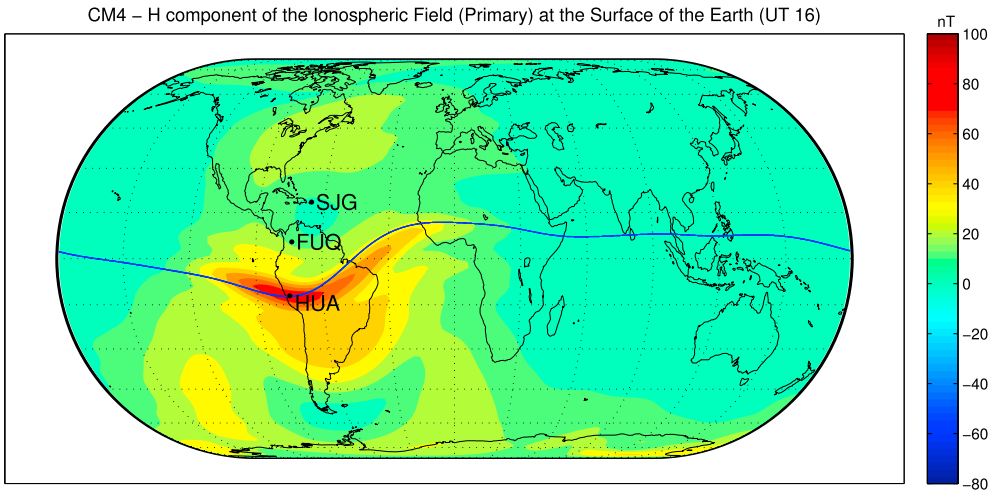

Figure 1. Geomagnetic field variations at the Earth's surface caused by ionospheric current as derived using the CM4 model at 16 UT on the first day of the year with $F_{10.7}$ = 100 sfu. The black dots mark the considered observatory locations. The blue line represents the dip equator latitude.

To estimate the EEJ strength using a reference station, we first subtract the quiet nighttime values from the recorded *H* data for both the equatorial and the reference station to remove the effects of the main field.

$$\Delta H = H - H_{\mathrm{MF}} \tag{1}$$

ΔH reflects the daily variation with respect to the local midnight baseline. H_{MF} is computed daily using the mean of the four nighttime values of *H* at 23:30, 00:30, 01:30, and 02:30 LT. Then, H_{EEJ} is estimated by computing the difference between the daily variations at the equatorial and the reference station.

$$H_{\mathrm{EEJ}} = \Delta H_{\mathrm{EEJ}} - \Delta H_{\mathrm{NonEEJ}} \tag{2}$$

The underlying assumption behind the differencing is that the large-scale fields of magnetospheric currents are expected to be approximately equal at both observatories [e.g., *Manoj et al.*, 2006]. A part of the S_q contributions at the equatorial observatory is also removed by this method.

In the second approach the H_{EEJ}, which is proportional to the EEJ strength, is estimated by subtracting the disturbance index *Dst* from the recorded *H* data at the equatorial observatory to account for the effects of the ring current. Then, H_{EEJ} is estimated after subtracting the quiet nighttime value. The S_q contributions at the equatorial observatory are not removed in this method.

In this paper we attempt to compare the semimonthly lunar tidal amplitudes estimated from the Huancayo data by using both these methods for the period 1997–2013. San Juan and Fuquene have been chosen as reference stations for Huancayo. Figure 1 shows the geomagnetic field variation due to the primary ionospheric (excluding induced) currents at the Earth's surface as derived from the CM4 model at 16 UT on 1 January 2000. The black dots mark the locations of the three observatories used in this study. CM4 (Comprehensive Model) is a model of the quiet-time, near-Earth magnetic field which has been derived using the POGO, Magsat, Ørsted and CHAMP satellite data [*Sabaka et al.*, 2004].

The significant difference in latitudinal separation from the magnetic equator also provides a chance to look at the dependence of the lunar tidal amplitudes on the spatial distance between the equatorial and the reference stations.

The EEJ has a strong dependence on the solar flux level due to varying ionospheric conductivity [e.g., *Alken and Maus*, 2007; *Stolle et al.*, 2008; *Yamazaki et al.*, 2010]. To eliminate the effect of the varying conductivity, the EEJ strength is normalized to a solar flux level of 150 sfu. The data are then arranged into bins of 1 day by 1 h in local time (LT) over a period of two lunar months (59 days). For each day, a 59 day centered sliding window is applied. The local time sector considered here is from 08:00 to 16:00 LT. Outside of this time interval the EEJ

signal is considered to be weak. The daytime variation of the EEJ is dominated by the solar tidal effects. This dominant variation is estimated by calculating the means over a 59 day period for each local time hour. The calculated means are then subtracted from the data to remove the effect of the solar tides. We are interested in estimating the amplitude of the semimonthly lunar wave (14.77 days) for each local time hour over the 59 day period. The frequency of interest is the fourth harmonic signal for which the amplitude and phase are determined for each local time hour. The amplitude obtained is then normalized for the expected diurnal variation of the ionospheric conductivity, C, as described by *Lühr et al.* [2008].

$$C = C_0 \sqrt{\cos\left\{\frac{\pi}{12\ \mathrm{h}}(\mathrm{LT} - t_0)\right\}} \tag{3}$$

where C_0 is the value of the peak conductivity and t_0 is the local time of the peak conductivity. A suitable value for t_0 has been found to be 12:30 LT. For our purpose we chose C_0 to be equal to 1.

The procedure for normalization is similar to the one explained in *Siddiqui et al.* [2015]. It has been shown by *Lühr et al.* [2012] that the diurnal variation of the ionospheric conductivity also affects the amplitude of the lunar tidal signal. Without the normalization, the values around noon would dominate the tidal results.

A reasonable estimate of the average semimonthly lunar wave over 59 days was obtained by calculating the mean of the normalized amplitudes for all the considered local times. The mean semimonthly lunar wave is thus computed for each 59 day window and is then tied to its central day. A sliding window of 59 days length advanced by 1 day is applied for each subsequent data set.

3.2. Quantifying SSW Strength Based on Polar Vortex Weakening

Lately, various studies on the enhanced lunar response of the ionosphere during SSWs have used different diagnostics to identify an SSW event. *Yamazaki* [2013] used the NCEP/NCAR reanalysis data to recognize SSW events based on significant changes in the climatology of the stratosphere dynamics, whereas *Zhang and Forbes* [2014] quantified the concept of polar vortex weakening (PVW) to characterize the strength of SSW events using the MERRA reanalysis data. Based on SABER V2.0 temperature measurements between ±50° latitude, they demonstrated a correlation between the timing and peak amplitude of the M_2 at 110 km altitude and the polar vortex weakening.

Chau et al. [2015] used this definition of PVW to demonstrate a correlation between the upper mesospheric lunar tides and PVW characteristics during SSW events. However, they have also reported inconsistencies for some years [see *Chau et al.*, 2015, Figure 7] when the mesospheric lunar tides are enhanced prior to the PVW day as identified by *Zhang and Forbes* [2014].

Zhang and Forbes [2014] have used the daily time series of the zonal mean zonal wind (U) at 70°N and 48 km altitude and zonal mean temperature (T) at North Pole and 40 km altitude for the first 60 days of each year to describe the polar vortex weakening (see Figure 2) [*Zhang and Forbes*, 2014]. In our study we extend the time series for both parameters from 60 to 90 days by including the month of December. Figure 2 presents U (red curve) and T (black curve) as defined above from December onward to February for the years 1998–2013. The dotted blue vertical lines denote the days of peak polar vortex weakening, while the dotted black horizontal lines denote the zero value of mean zonal wind. The dotted vertical green line in each panel marks the day of peak lunar tidal enhancement estimated from the magnetometer data. The PVW events are identified according to the same criteria as used by *Zhang and Forbes* [2014] by locating the most significant and/or earliest pair of T and U extremes within these 90 days. Though, the PVW event of 2000 was not included in their analysis, we have included the event as it fulfills the criteria used for identifying PVWs. For the years 2005 and 2007, PVWs are not well defined. It is important to note that our results for the occurrence of PVW events are only different for the years 1998, 1999, 2001, and 2002 from the results of *Zhang and Forbes* [2014]. During these periods the earliest T and U extremes were recorded during December. For the rest of the years between 1998 and 2013 we obtain the same PVW days as reported by them.

The strength of PVW is better represented by the peak magnitude of the reversed mean zonal wind than the zonal mean of the stratospheric temperature according to the results of *Zhang and Forbes* [2014]. The magnitude of extreme values of the reversed mean zonal wind is taken as the measure of PVW strength and is denoted by PVW_mag. The magnitude and the occurrence date of PVWs for the years 1998–2013 are listed in Table 1.

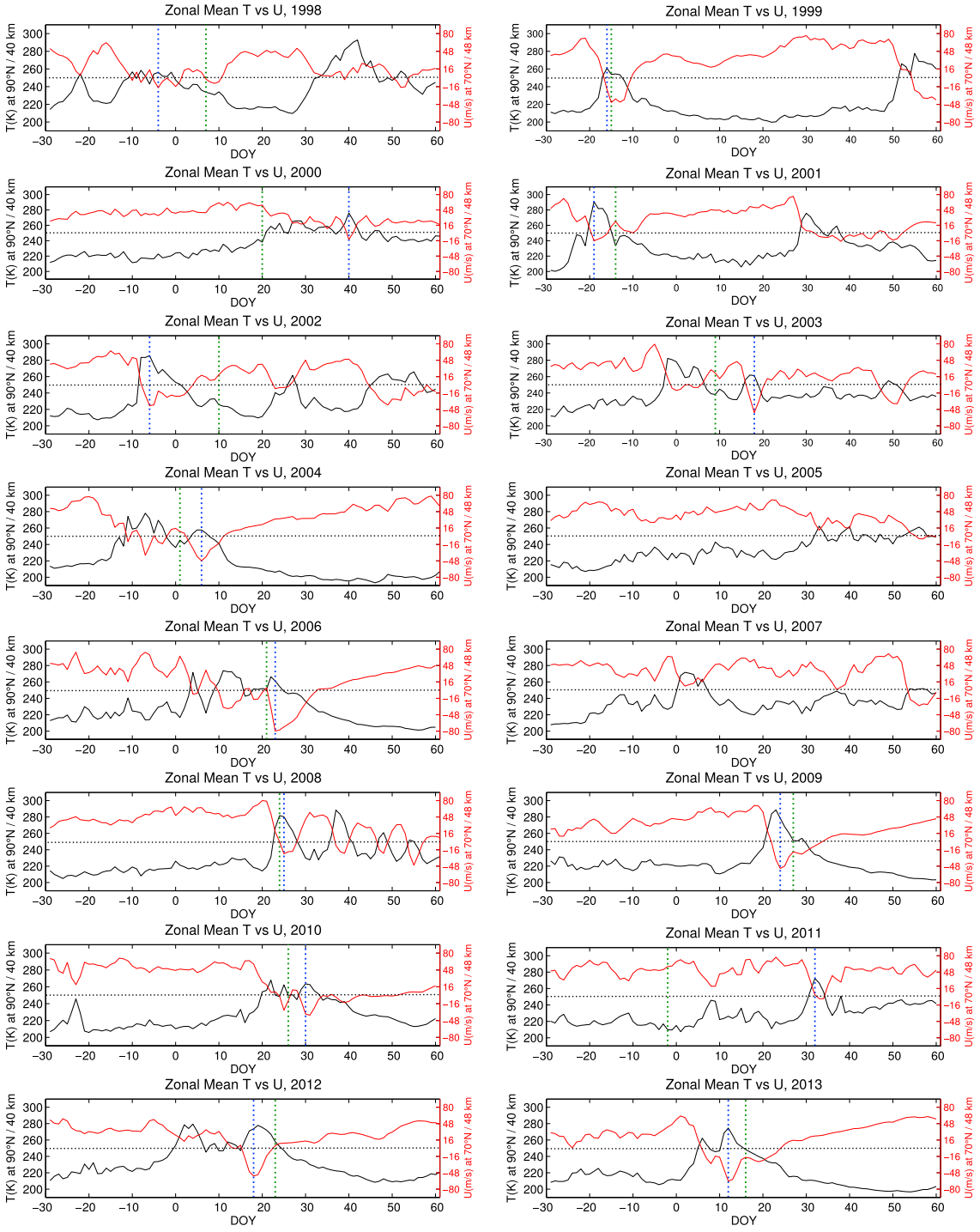

Figure 2. Daily time series of the mean zonal wind (U) at 70°N and 48 km altitude (red curve) and zonal mean temperature (*T*) at North Pole and 40 km (black curve) from December onward to February for the years 1998–2013. The dotted vertical blue line in each panel marks the selected polar vortex weakening day. The dotted vertical green line in each panel marks the day of peak lunar tidal enhancement.

4. Observation

Figure 3 shows the lunar tidal power obtained solely from Huancayo observations for the years 1997–2013. The red lines denote the peak PVW days as identified in Figure 2. The annual amplification of the lunar tidal power can be seen in all these years during the months of December–February with a magnitude of at least 600 nT^2. The peak amplification for a majority of the years occurs around the PVW day if a PVW has been

Table 1. The Date and Strength of Polar Vortex Weakening (PVW) Events Derived From MERRA Reanalysis Data for the Years 1998–[a]

Date of PVWs	PVW Strength (ms^{-1})
26/12/1998	17.68
15/12/1999	44.57
8/2/2000	13.45
11/12/2000	16.12
24/12/2001	40.68
17/1/2003	54.21
5/1/2004	47.71
22/1/2006	79.78
24/1/2008	23.75
23/1/2009	52.42
29/1/2010	37.92
31/1/2011	3.78
17/1/2012	54.33
11/1/2013	64.31

[a]The strength of PVWs is represented by the magnitude of the westward zonal mean zonal wind at 70°N/48 km altitude. Dates are formatted as day/month/year.

identified. For the four largest events (2003, 2006, 2009, and 2013) with amplitudes of lunar wave power above 1500 (nT^2) we also identified PVW strengths above 50 ms^{-1} (See Table 1). The next large enhancement, in 2008, shows only a small amplitude of PVW with 23.75 ms^{-1}; however, it is influenced by multiple warming events at least up to the end of February. This suggests that the recurrence could be responsible for the large lunar wave amplitude seen in the semimonthly lunar tide. Large M_2 temperature amplitudes during the years 2006, 2009, and 2013 were also reported by *Zhang and Forbes* [2014]. We also find cases of lunar tidal enhancements without significant PVW in the years 2005 and 2007 exhibiting similar amplitudes as in the years 2001, 2002, 2011, and 2012 with significant PVW. This suggests that there are other physical processes responsible for the lunar tidal enhancements in the EEJ that needs to be further investigated. Such counterexamples were earlier reported by *Siddiqui et al.* [2015]. We do not find a one-to-one correspondence between the timing of lunar tidal amplification and the PVW. The breakdown of a one-to-one correspondence between the lunar tidal enhancements and the warming events for certain years was also observed by *Stening* [2011] and *Yamazaki et al.* [2012].

Figures 4 and 5 show the lunar tidal power obtained by using San Juan and Fuquene as reference stations, respectively. Similar amplifications during the major warming events are observed in both these plots. With Fuquene as the reference station the lunar tidal signature for the years 1997–2011 is slightly clearer compared to San Juan. It can be seen in the former case that the sidebands in general have lower amplitudes compared to the latter. Also, in case of the 2001 event, the lunar enhancement correlates better with the PVW when Fuquene is the reference station for Huancayo. This could be due to the larger latitudinal and longitudinal separation between Huancayo and San Juan compared to Huancayo and Fuquene. The contributions from the S_q current system are better eliminated when calculating the EEJ strength with respect to Fuquene as reference station than San Juan, since the latter lies close to the S_q focus with the values of H component recordings being close to zero. However, the overall lunar tidal pattern obtained from the Huancayo-Fuquene

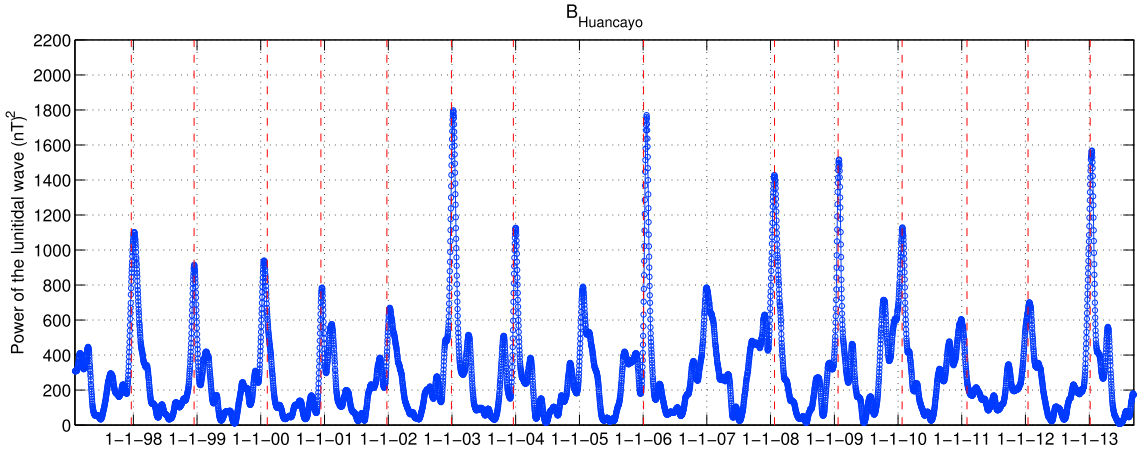

Figure 3. Daily EEJ lunar tidal wave power for the years 1997–2013. Results are obtained without a reference station to Huancayo. The red lines denote the PVW days derived from the reversed zonal wind (see text).

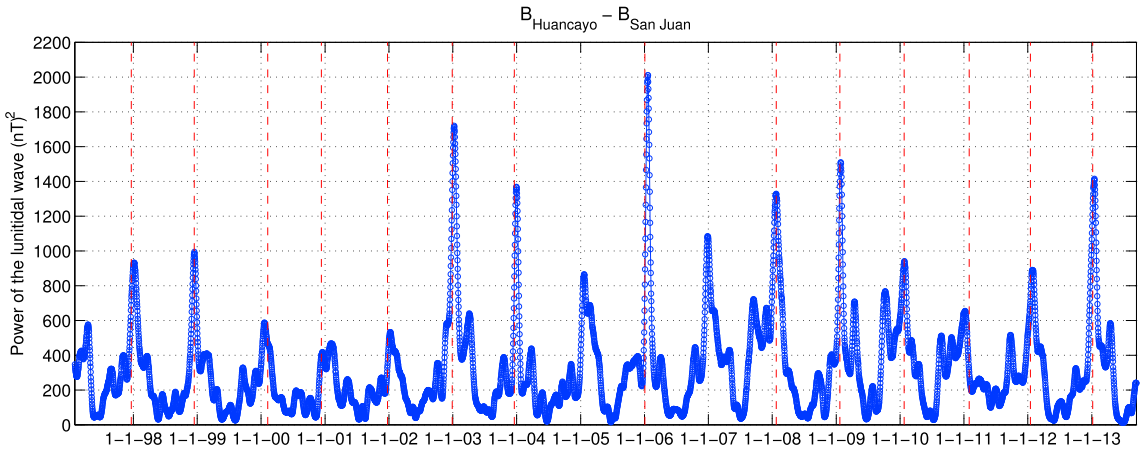

Figure 4. Same as Figure 3 but with San Juan as the reference station for Huancayo.

pair, Huancayo-San Juan pair, and solely from Huancayo suggest that the semimonthly lunar tidal amplitude in the EEJ is dominant over the lunar tidal amplitude in the S_q currents.

The *H* component data from Fuquene are presently only available till 2011. Moreover, occasional gaps in Figure 5 result due to the data gaps at the Fuquene station.

5. Discussion

In order to quantify our observations, we now present the correlations between the timing and amplitude of PVW and the semimonthly lunar tide in the EEJ. Figure 6 presents the scatter plot between the occurrence day of PVWs and the semimonthly lunar tidal peaks during 1998–2013 for Huancayo. The points depicted with the square symbol correspond to the years when the lunar tidal maximum occurred significantly earlier than the defined PVW day for that year. The solid red line depicts the linear least squares fit to the events. The lunar tidal amplification occurs much earlier than the defined PVW day for the 2000 and 2011 events. The mismatch between the occurrence of the PVW and the M_2 lunar tide derived from MLT winds was also reported by *Chau et al.* [2015] in case of the 2011 event. These are the only two years remaining for which the revised definition of PVW (by including December) could not improve the temporal relation between the PVW and the lunar tidal enhancement in the magnetic data. The slope of the linear fit is 0.79. It is slightly lower than 0.92, as obtained by *Chau et al.* [2015] when they estimated the lunar tide in the upper mesospheric winds from a midlatitude station while *Zhang and Forbes* [2014] reported a unity slope. They showed with the SABER temperature measurements at 110 km altitude that it took 2.8 days for the M_2 tide to respond to PVW. It can be seen in Figure 6 that the difference between the occurrence of lunar tidal peaks and PVWs in January is less than 3 days in six out of nine cases. For the 2003 and 2004 events the lunar peaks occurred even earlier than

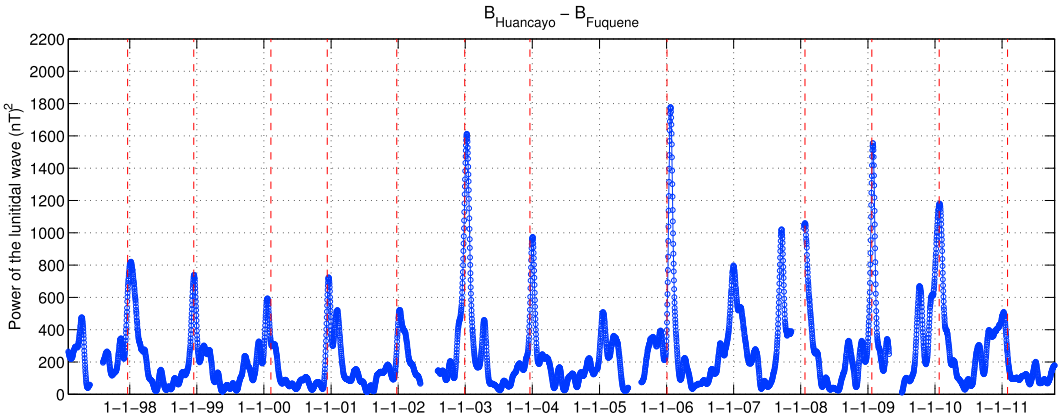

Figure 5. Same as Figure 3 but with Fuquene as the reference station for Huancayo.

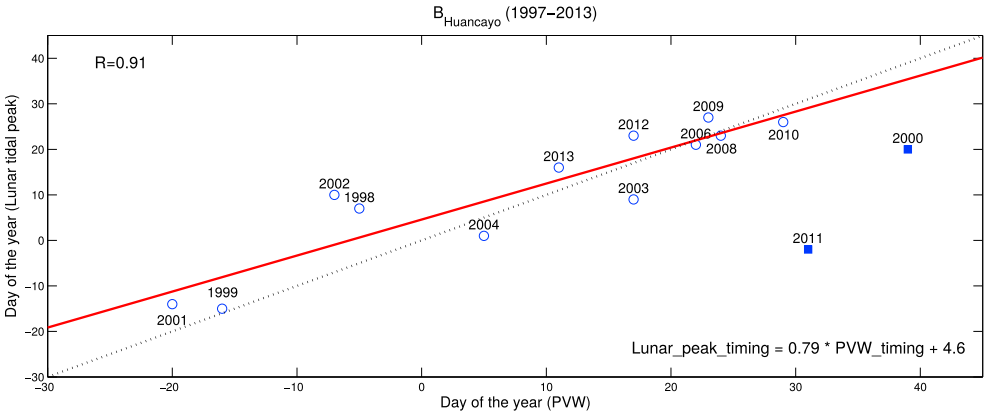

Figure 6. The figure presents a scatter plot between the occurrence days of PVW and EEJ semimonthly lunar tidal peak during 1997–2013 for Huancayo. The filled squares correspond to the years when the lunar tidal maximum occurred much earlier than the selected PVW day for that year. The solid red line depicts the linear least squares fit to the events. The equation for the fit and the correlation coefficient are listed in the panel. The dotted black line represents the one-to-one correspondence.

the identified PVW days. These events record multiple reversals of the zonal wind prior to the identified PVW days which might have triggered the early enhancement of the lunar tides. Delayed response of lunar peaks to PVWs can be found for the December events of 1998 and 2002. From the linear regression between the occurrence of the PVW event and the peak of the semimonthly lunar tidal amplitude we derive an equation

$$M_2\_\text{peak\_timing} = 0.79\,\text{PVW\_timing} + 4.6\,(\text{days}) \tag{4}$$

where, M_2_peak_timing is the day of peak semimonthly lunar tidal amplitude and PVW_timing is the identified PVW day. The slope of less than 1 is caused by the delayed response of the tidal enhancement (10–20 days) for PVWs occurring in December. It should be checked which processes cause these delays. When ignoring the December events in Figures 6–8, a unity slope (not shown here), as reported by *Zhang and Forbes* [2014], is justified.

The value of the correlation coefficient obtained compares excellently with the values reported by *Zhang and Forbes* [2014] and *Chau et al.* [2015], even though they derived the lunar tidal enhancements from completely different quantities. Our results thus support their observations and further demonstrate that the response of the upper atmosphere to PVW events compares well on a global scale, i.e., at low, middle, and high latitudes. Analyses at these three latitudinal regimes have been performed with ground-based observations of MLT winds at middle and high latitudes [*Chau et al.*, 2015] and with observations of the *E* region dynamo between ±50° latitude [*Zhang and Forbes*, 2014]. It is noteworthy that similar results have been achieved in these analyses with different parameters of the upper atmosphere and at different latitudes.

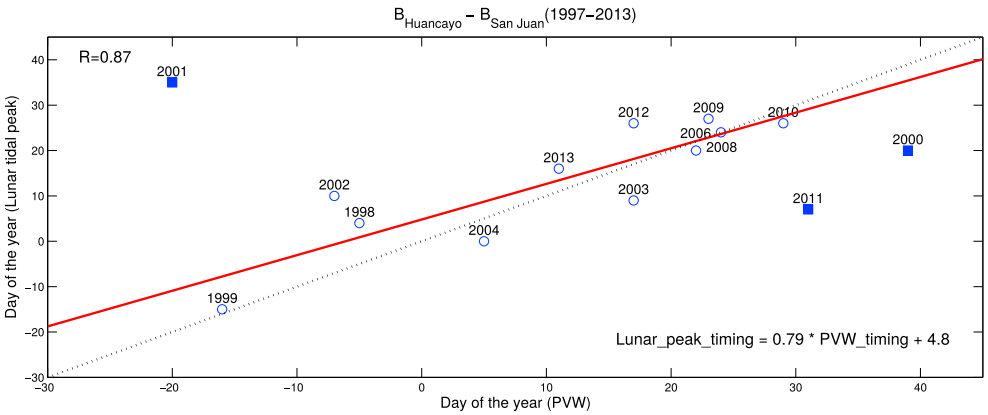

Figure 7. Same as Figure 6 but with San Juan as the reference station for Huancayo.

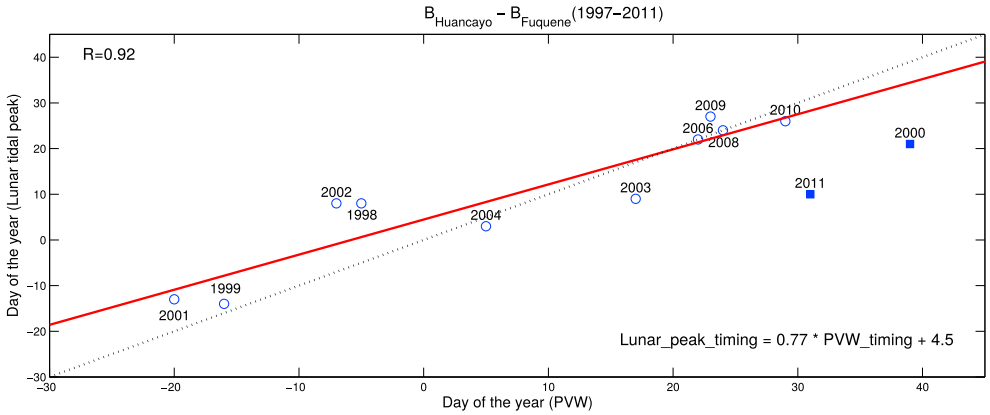

Figure 8. Same as Figure 7 but with Fuquene as the reference station for Huancayo.

Figures 7 and 8 present the same scatter plots as in Figure 6 but for cases when San Juan or Fuquene have been used as a reference station for Huancayo. The slopes and the correlation coefficients are similar to the results obtained from the single-station method. The largest correlation coefficient of 0.92 is obtained when Fuquene is considered as the reference station for Huancayo. With San Juan as the reference station the correlation coefficient is 0.87, whereas it is 0.91 when the single-station method is considered.

Figure 9 presents the scatter plot between the PVW strength and the peak of the EEJ lunar tidal amplitude at Huancayo. The lunar tidal amplitude is considered in Figures 9–11 instead of the lunar tidal power, in order to maintain consistency with the results of *Chau et al.* [2015] and *Zhang and Forbes* [2014]. The solid red line depicts the linear least squares fit to the events. The dotted black horizontal and vertical lines mark a chosen threshold level for the lunar amplitude and PVW strength during major warmings. The 2000 and 2011 events are not included in the analysis due to the large difference between the occurrence time of PVW and the lunar tidal peak for these cases. In general, larger lunar tidal amplitudes correlate with stronger PVW strength. During the four major SSW events (2003, 2006, 2009, and 2013) the amplitude of the lunar tide is greater than 35 nT, and the PVW strength is greater than 50 ms^{-1}. In case of the 2012 event, a low amplitude of the lunar tide is obtained in spite of a similar value of PVW strength as during major warmings. However, our results are consistent with the observations of *Zhang and Forbes* [2014] and *Chau et al.* [2015] where they have also reported lower amplitude of the M_2 lunar tide for this particular event. This observation is discussed later in more detail in this section.

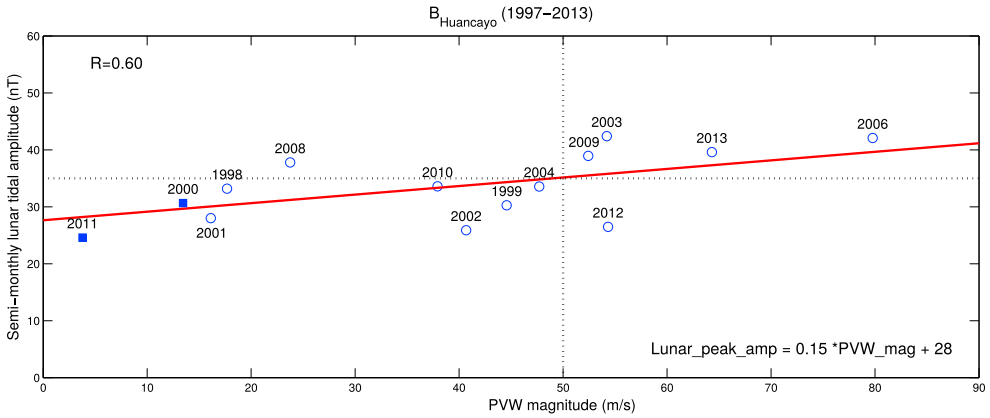

Figure 9. The figure presents a scatter plot between the strength of PVW and the peak amplitude of the semimonthly lunar tidal peak during 1997–2013 for Huancayo. The filled squares correspond to the years when the lunar tidal maximum occurred much earlier than the selected PVW day for that year. The solid red line depicts the linear least squares fit to the events. The equation for the fit and the correlation coefficient are listed in the panel. The dotted black horizontal and vertical lines mark the threshold values for the lunar amplitude and PVW strength during major warmings.

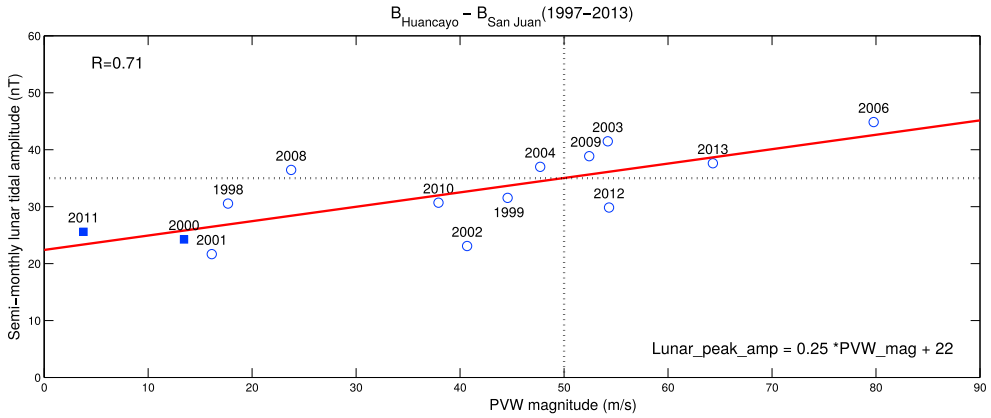

Figure 10. Same as Figure 9 but with San Juan as the reference station for Huancayo.

Figures 10 and 11 present the scatter plot between the PVW strength and the lunar tidal amplitude when San Juan and Fuquene are used as the reference station for Huancayo. As seen from the earlier plot, stronger PVW strength leads to larger lunar tidal amplitudes in these cases too. Slightly higher correlation is achieved between the PVW strength and the peak of the lunar tidal amplitude by using the reference station method in comparison to the single-station method. The largest correlation coefficient of 0.75 is obtained when Fuquene is considered as the reference station for Huancayo and it is 0.71 in the case of San Juan. When the single-station method is used, the value of the correlation coefficient obtained is 0.60 and the lowest among the three cases. We expect a better separation of EEJ from S_q and magnetospheric fields when Fuquene is the reference station for Huancayo compared to San Juan.

From the linear regression between the reversed zonal wind speed and the semimonthly lunar tidal amplitude we derive the equation

$$M_2\_\text{peak\_amplitude} = 0.25\left(\frac{\text{nT}}{\text{ms}^{-1}}\right)\text{PVW\_mag} + 22\,(\text{nT}) \tag{5}$$

where the peak magnitude of PVW, PVW_mag, is given in ms^{-1} and the peak amplitude of the semimonthly lunar tide, M_2_peak_amplitude, is given in nT. From Figures 9 to 11 we see that the 2000 and 2011 events exhibit the smallest amplitudes. This may correspond to our findings that they appear as outliers for the timing in Figures 6–8.

The inconsistencies observed during the 2000, 2011, and the 2012 events could be better explained if the different external factors which influence the occurrence of the SSWs and the strength of the polar vortex such as the tropospheric wave activity, the 11 year sunspot cycle, the phase of the QBO (quasi-biennial oscillation) [e.g., *Holton and Tan*, 1980; *Labitzke and Van Loon*, 1988; *Van Loon and Labitzke*, 2000], and the phase of the El Niño–Southern Oscillation (ENSO) [e.g., *Butler and Polvani*, 2011] are also taken into account. The SSWs

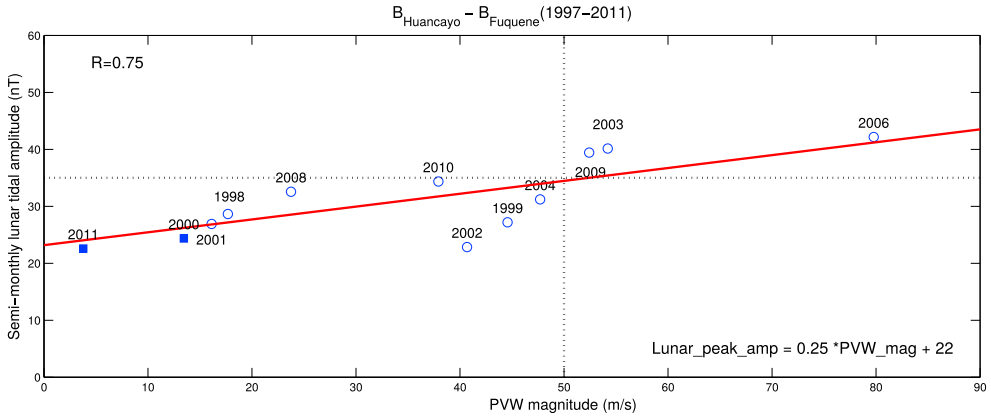

Figure 11. Same as Figure 9 but with Fuquene as the reference station for Huancayo.

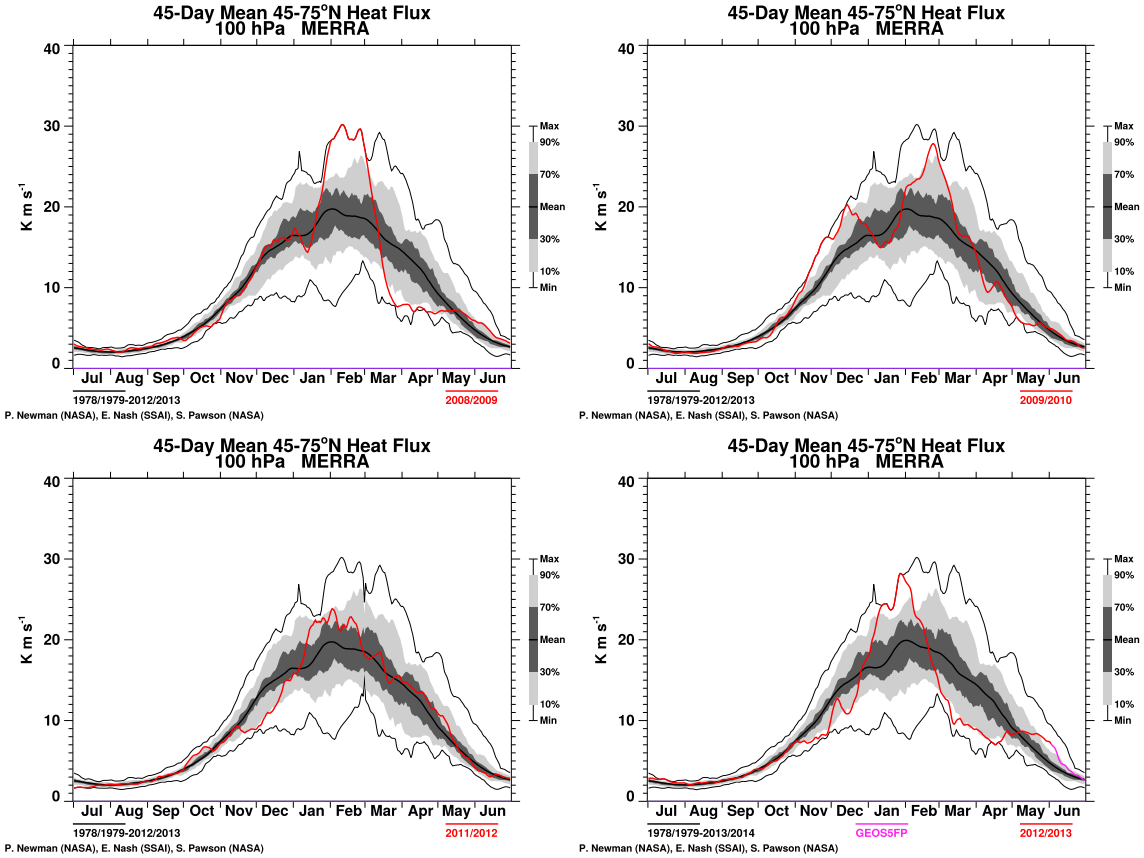

Figure 12. The 45 day mean of the 45°N–75°N averaged eddy heat flux at 100 hPa denoted by red lines (top row) for the years 2008/2009 and 2009/2010 and (bottom row) for the years 2011/2012 and 2012/2013. The bold black line in each panel denotes the climatological mean of the eddy heat flux calculated over the period from 1978/1979 to 2012/2013. Images courtesy of NASA GSFC http://ozonewatch.gsfc.nasa.gov/meteorology/NH.html.

are more likely to occur under the solar minimum conditions during the east phase of the QBO and under solar maximum conditions during the west phase of the QBO [*Labitzke*, 2005]. The SSWs also occur twice as frequently during the El Niño and La Niña winters as compared to ENSO-neutral winters, although the probability of occurrence is almost equal during both El Niño and La Niña winters [*Butler and Polvani*, 2011]. The 2003 SSW event was characterized by the west phase of QBO under strong solar flux conditions together with the El Niño phase of the ENSO. Under these conditions the Brewer-Dobson circulation (BDC) is enhanced which leads to a weakened and warm polar vortex [e.g., *Labitzke*, 2005; *Butler and Polvani*, 2011]. The 2006 SSW event was characterized by the east phase of the QBO during solar minima and with La Niña phase of the ENSO. These conditions also enhance the Brewer-Dobson circulation (BDC) which facilitates the occurrence of SSWs.

During the 2009 SSW event the conditions were favorable for an undisturbed and strong polar vortex [*Labitzke and Kunze*, 2009], because the event was characterized by a minima in solar cycle together with the west phase of the QBO. However, due to the large tropospheric forcing (estimated using the eddy heat flux value at 100 hPa) which was among the three strongest recorded since 1958 [*Ayarzagüena et al.*, 2011], the stratospheric warming occurred. The eddy heat flux at 100 hPa averaged over 45°N–75°N is regarded as a measure of the amount of wave activity entering the stratosphere [e.g., *Waugh et al.*, 1999; *Newman et al.*, 2001; *Polvani and Waugh*, 2004]. Figure 12 presents the 45 day mean of the 45°N–75°N averaged eddy heat flux at 100 hPa denoted by red lines for the years 2008/2009 and 2009/2010 in the top row and for the years 2011/2012 and 2012/2013 in the bottom row. The bold black line in each panel denotes the climatological mean calculated over the period from 1978/1979 to 2012/2013. The enhanced eddy flux values during the 2009 SSW event can be clearly seen in Figure 12.

The 2013 event was characterized by the east phase of the QBO under moderate solar flux conditions and the neutral phase of the ENSO. However, the 2013 SSW event also witnessed a strong tropospheric forcing albeit

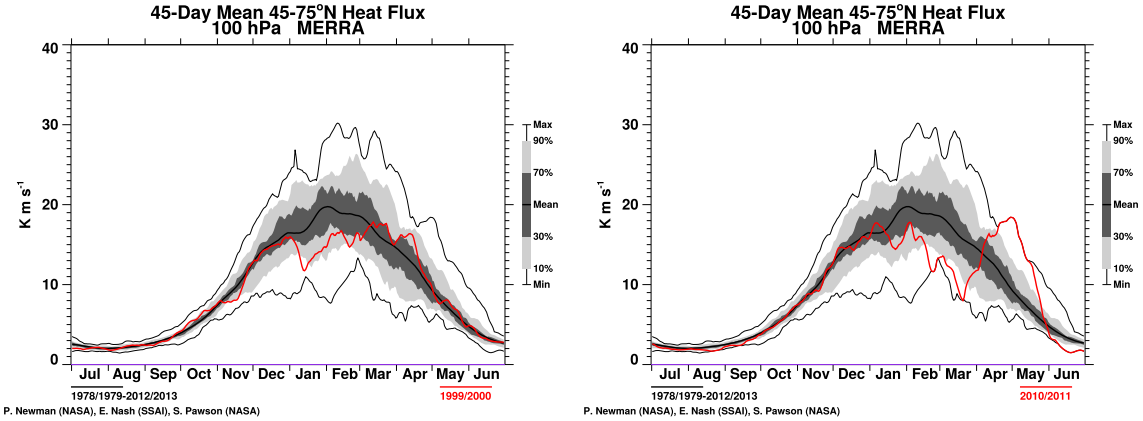

Figure 13. Same as Figure 12 but for the years (left) 1999/2000 and (right) 2010/2011.

slightly lesser than the 2009 SSW event [*Coy and Pawson*, 2015] which may have led to the splitting of the polar vortex.

The lower atmosphere and ionosphere coupling around SSWs is not directly related to the warming itself but to the Planetary Wave (PW) activity associated with it [*Chau et al.*, 2012]. In the case of the 2012 SSW event, the lunar tidal enhancement was low in comparison to the magnitude of vortex weakening. During this event a weaker level of tropospheric forcing than the 2009 and the 2013 events (as seen in Figure 12 through the averaged eddy heat flux values) was witnessed, even though the magnitude of PVWs were comparable. The 2012 SSW event was characterized by the east phase of QBO during solar minima with the La Niña phase of the ENSO. Under these conditions a weak polar vortex is expected. The relatively lower level of tropospheric forcing combined with the weakened polar vortex could be the reasons for the low values of the semimonthly lunar tide in the EEJ, although the magnitude of PVW during the 2012 minor SSW event was large.

Figure 13 presents the 45 day mean of the 45°N–75°N averaged eddy heat flux at 100 hPa denoted by red lines for the years 1999/2000 (Figure 13, left) and 2010/2011 (Figure 13, right). The averaged eddy heat flux value at 100 hPa recorded during the 2000 and 2011 boreal winters were lower than the climatological mean (bold black lines), and the lunar tidal enhancement for these years do not seem to be related to the PVW. The existence of these cases suggests that there are also other physical processes which are responsible for the lunar tidal enhancements that are not covered in our discussion.

Although the results obtained by *Zhang and Forbes* [2014] and *Chau et al.* [2015] were based on the lunar tidal measurements of different atmospheric quantities and heights, yet our observations are in general agreement with the ones reported by them. We suggest that the M_2 signatures identified in mesospheric winds by *Chau et al.* [2015] should be compared to the semimonthly lunar signature in the EEJ caused by the *E* region dynamo.

6. Conclusions

Using the *H* component data from Huancayo, San Juan, and Fuquene, we have compared (a) the lunar tidal modulation of the EEJ for the years 1997–2013 based on two different approaches for the elimination of magnetospheric contribution and (b) the lunar tidal modulation of the EEJ estimated with and without the S_q contributions to the EEJ. The peak of the derived semimonthly lunar tides are then compared with the timing and magnitude of the stratospheric polar vortex weakening (PVW). Major points of our study are as follows:

1. We determined correlation coefficients and linear regression functions when comparing timing or amplitude relations between PVW and peak lunar tidal amplitudes for the following cases: using Huancayo observatory data only, Huancayo data with a reference station located equatorward of the S_q focus (Fuquene), and with a reference station located close to the S_q focus (San Juan). These observations suggest that the variations of the EEJ in response to PVW events to a large degree determine the observed variations of the total current (EEJ + S_q), which is the sum of both the EEJ and S_q at the magnetic equator.
2. Our results show a good qualitative agreement with the observations of *Zhang and Forbes* [2014] and *Chau et al.* [2015]. We obtain an improved correlation between the timings of PVW and lunar tidal peaks when

the month of December is also included in the analysis. Similarly, we find a direct relation between the peak amplitude of the semimonthly lunar tide and the peak magnitude of the PVW.

3. The timing of the PVW events and the peak timing of the lunar tidal amplitude seem to be related closer to each other than the amplitudes of both quantities. This is demonstrated by higher correlation coefficients of about 0.9 between the two parameters for the timing and 0.75 for the amplitudes. Although many different parameters of the upper atmosphere system influence the amplitude of the EEJ lunar tidal modulation, the commencement of a lunar tidal enhancement in most cases is closely related to a PVW event.
4. The external factors affecting the state of the wintertime northern polar vortex such as the QBO, solar flux levels, ENSO, and the tropospheric forcing levels have also been considered to explain the weak lunar tidal enhancements in the EEJ. However, other parameters that could not be covered in our work have to be considered in the future to explain all the observations consistently.

Acknowledgments

The results presented in this paper rely on the data collected at San Juan, Fuquene, and Huancayo. We thank the INTERMAGNET for promoting high standards of magnetic observatory practice and the U.S. Geological Survey and the Instituto Geofisico del Peru for supporting geomagnetic observatory operations at San Juan and Huancayo, respectively. We thank the Instituto Geográfico Agustin Codazzi, Colombia, for supporting geomagnetic observatory operations at Fuquene. We employ data from MERRA (Modern-Era Retrospective Analysis for Research and Applications). The data are downloaded from ftp://goldsmr3.sci.gsfc.nasa.gov/data/s4pa/MERRA/. We are very thankful to WDC for Geomagnetism, Kyoto, for making available the *Dst* indices. The OMNI data for $F_{10.7}$ were obtained from the GSFC/SPDF OMNIWeb interface at http://omniweb.gsfc.nasa.gov. T.A.S. and C.S. thank the International Space Science Institute (ISSI) for organizing the team on "A three-dimensional ground-to-space understanding of sudden stratospheric warmings" and for sponsoring the team meetings on this research topic.

References

Alken, P., and S. Maus (2007), Spatio-temporal characterization of the equatorial electrojet from CHAMP, Ørsted, and SAC-C satellite magnetic measurements, *J. Geophys. Res.*, *112*, A09305, doi:10.1029/2007JA012524.

Andrews, D. G., J. R. Holton, and C. B. Leovy (1987), *Middle Atmosphere Dynamics*, vol. 40, Academic Press, San Diego, Calif.

Ayarzagüena, B., U. Langematz, and E. Serrano (2011), Tropospheric forcing of the stratosphere: A comparative study of the two different major stratospheric warmings in 2009 and 2010, *J. Geophys. Res.*, *116*, D18114, doi:10.1029/2010JD015023.

Baldwin, M. P., and T. J. Dunkerton (2001), Stratospheric harbingers of anomalous weather regimes, *Science*, *294*(5542), 581–584, doi:10.1126/science.1063315.

Bartels, J., and H. Johnston (1940), Geomagnetic tides in horizontal intensity at Huancayo, *Terr. Magn. Atmos. Electr.*, *45*(3), 269–308, doi:10.1029/TE045i003p00269.

Butler, A. H., and L. M. Polvani (2011), El Niño, La Niña, and stratospheric sudden warmings: A reevaluation in light of the observational record, *Geophys. Res. Lett.*, *38*, L13807, doi:10.1029/2011GL048084.

Butler, A. H., D. J. Seidel, S. C. Hardiman, N. Butchart, T. Birner, and A. Match (2015), Defining sudden stratospheric warmings, *Bull. Am. Meteorol. Soc.*, doi:10.1175/BAMS-D-13-00173.1, in press.

Charlton, A. J., and L. M. Polvani (2007), A new look at stratospheric sudden warmings. Part I: Climatology and modeling benchmarks, *J. Clim.*, *20*(3), 449–469, doi:10.1175/JCLI3996.1.

Chau, J. L., L. P. Goncharenko, B. G. Fejer, and H.-L. Liu (2012), Equatorial and low latitude ionospheric effects during sudden stratospheric warming events, *Space Sci. Rev.*, *168*(1–4), 385–417.

Chau, J. L., P. Hoffmann, N. M. Pedatella, V. Matthias, and G. Stober (2015), Upper mesospheric lunar tides over middle and high latitudes during sudden stratospheric warming events, *J. Geophys. Res. Space Physics*, *120*, 3084–3096, doi:10.1002/2015JA020998.

Coy, L., and S. Pawson (2015), The major stratospheric sudden warming of January 2013: Analyses and forecasts in the GEOS-5 data assimilation system, *Mon. Weather Rev.*, *143*(2), 491–510, doi:10.1175/MWR-D-14-00023.1.

Forbes, J. M., and X. Zhang (2012), Lunar tide amplification during the January 2009 stratosphere warming event: Observations and theory, *J. Geophys. Res.*, *117*, A12312, doi:10.1029/2012JA017963.

Holton, J. R., and H.-C. Tan (1980), The influence of the equatorial quasi-biennial oscillation on the global circulation at 50 mb, *J. Atmos. Sci.*, *37*(10), 2200–2208.

Labitzke, K. (2005), On the solar cycle–QBO relationship: A summary, *J. Atmos. Sol. Terr. Phys.*, *67*(1), 45–54, doi:10.1016/j.jastp.2004.07.016.

Labitzke, K., and M. Kunze (2009), On the remarkable Arctic winter in 2008/2009, *J. Geophys. Res.*, *114*, D00I02, doi:10.1029/2009JD012273.

Labitzke, K., and H. Van Loon (1988), Associations between the 11-year solar cycle, the QBO and the atmosphere. Part I: The troposphere and stratosphere in the Northern Hemisphere in winter, *J. Atmos. Terr. Phys.*, *50*(3), 197–206.

Limpasuvan, V., D. W. Thompson, and D. L. Hartmann (2004), The life cycle of the Northern Hemisphere sudden stratospheric warmings, *J. Clim.*, *17*(13), 2584–2596.

Lühr, H., M. Rother, K. Häusler, P. Alken, and S. Maus (2008), The influence of nonmigrating tides on the longitudinal variation of the equatorial electrojet, *J. Geophys. Res.*, *113*, A08313, doi:10.1029/2008JA013064.

Lühr, H., T. A. Siddiqui, and S. Maus (2012), Global characteristics of the lunar tidal modulation of the equatorial electrojet derived from CHAMP observations, *Ann. Geophys.*, *30*(3), 527–536, doi:10.5194/angeo-30-527-2012.

Manoj, C., H. Lühr, S. Maus, and N. Nagarajan (2006), Evidence for short spatial correlation lengths of the noontime equatorial electrojet inferred from a comparison of satellite and ground magnetic data, *J. Geophys. Res.*, *111*, A11312, doi:10.1029/2006JA011855.

Martineau, P., and S.-W. Son (2013), Planetary-scale wave activity as a source of varying tropospheric response to stratospheric sudden warming events: A case study, *J. Geophys. Res. Atmos.*, *118*, 10,994–11,006, doi:10.1002/jgrd.50871.

Matsuno, T. (1971), A dynamical model of the stratospheric sudden warming, *J. Atmos. Sci.*, *28*(8), 1479–1494.

Newman, P. A., E. R. Nash, and J. E. Rosenfield (2001), What controls the temperature of the Arctic stratosphere during the spring?, *J. Geophys. Res.*, *106*(D17), 19,999–20,010.

Park, J., H. Lühr, M. Kunze, B. G. Fejer, and K. W. Min (2012), Effect of sudden stratospheric warming on lunar tidal modulation of the equatorial electrojet, *J. Geophys. Res.*, *117*, A03306, doi:10.1029/2011JA017351.

Polvani, L. M., and D. W. Waugh (2004), Upward wave activity flux as a precursor to extreme stratospheric events and subsequent anomalous surface weather regimes, *J. Clim.*, *17*(18), 3548–3554.

Sabaka, T. J., N. Olsen, and M. E. Purucker (2004), Extending comprehensive models of the Earth's magnetic field with Ørsted and CHAMP data, *Geophys. J. Int.*, *159*(2), 521–547, doi:10.1111/j.1365-246X.2004.02421.x.

Scherhag, R. (1952), Die explosionsartigen stratosphärenerwärmungen des spätwinters 1951/52, *Berichte des deutschen Wetterdienstes in der US-Zone*, *6*(38), 51–63.

Siddiqui, T. A., H. Lühr, C. Stolle, and J. Park (2015), Relation between stratospheric sudden warming and the lunar effect on the equatorial electrojet based on Huancayo recordings, *Ann. Geophys.*, *33*(2), 235–243, doi:10.5194/angeo-33-235-2015.

Stening, R. (2011), Lunar tide in the equatorial electrojet in relation to stratospheric warmings, *J. Geophys. Res.*, *116*, A12315, doi:10.1029/2011JA017047.

Stolle, C., C. Manoj, H. Lühr, S. Maus, and P. Alken (2008), Estimating the daytime Equatorial Ionization Anomaly strength from electric field proxies, *J. Geophys. Res.*, *113*, A09310, doi:10.1029/2007JA012781.

Van Loon, H., and K. Labitzke (2000), The influence of the 11-year solar cycle on the stratosphere below 30 km: A review, *Space Sci. Rev.*, *94*(1–2), 259–278, doi:10.1023/A:1026731625713.

Waugh, D. W., W. J. Randel, S. Pawson, P. A. Newman, and E. R. Nash (1999), Persistence of the lower stratospheric polar vortices, *J. Geophys. Res.*, *104*(D22), 27,191–27,201, doi:10.1029/1999JD900795.

Yamazaki, Y. (2013), Large lunar tidal effects in the equatorial electrojet during northern winter and its relation to stratospheric sudden warming events, *J. Geophys. Res.*, *118*, 7268–7271, doi:10.1002/2013JA019215.

Yamazaki, Y., K. Yumoto, T. Uozumi, S. Abe, M. G. Cardinal, D. McNamara, R. Marshall, B. M. Shevtsov, and S. I. Solovyev (2010), Reexamination of the S_q-EEJ relationship based on extended magnetometer networks in the east Asian region, *J. Geophys. Res.*, *115*, A09319, doi:10.1029/2010JA015339.

Yamazaki, Y., A. Richmond, and K. Yumoto (2012), Stratospheric warmings and the geomagnetic lunar tide: 1958–2007, *J. Geophys. Res.*, *117*, A04301, doi:10.1029/2012JA017514.

Zhang, X., and J. M. Forbes (2014), Lunar tide in the thermosphere and weakening of the northern polar vortex, *Geophys. Res. Lett.*, *41*, 8201–8207, doi:10.1002/2014GL062103.